JOURNAL OF COMPUTATIONAL PHYSICS 104, 457–469 (1993)

A Modified Chebyshev Pseudospectral Method with an $O(N^{-1})$ Time Step Restriction

DAN KOSLOFF

Department of Geophysical and Planetary Sciences, Raymond and Beverly Sackler Faculty of Exact Sciences, Tel-Aviv University, Tel-Aviv 69 978, Israel

AND

HILLEL TAL-EZER

Institute for Computer Applications in Science and Engineering and School of Mathematical Sciences, Raymond and Beverly Sackler Faculty of Exact Sciences, Tel-Aviv University, Tel-Aviv 69 978, Israel

Received September 12, 1989; revised April 26, 1991

The extreme eigenvalues of the Chebyshev pseudospectral differentiation operator are $O(N^2)$, where N is the number of grid points. As a result of this, the allowable time step in an explicit time marching algorithm is $O(N^{-2})$ which, in many cases, is much below the time step dictated by the physics of the PDE. In this paper we introduce a new differentiation operator whose eigenvalues are $O(N)$ and the allowable time step is $O(N^{-1})$. The new algorithm is based on interpolating at the zeroes of a parameter dependent, nonperiodic trigonometric function. The properties of the new algorithm are similar to those of the Fourier method but in addition it provides highly accurate solution for nonperiodic boundary value problems.

1. INTRODUCTION

Consider the first-order hyperbolic initial boundary value problem

$$u_t - u_x = 0, \qquad -1 < x < 1, \quad t \geqslant 0 \tag{1.1}$$

$$u(x, 0) = u^0(x), \qquad -1 < x < 1 \tag{1.2}$$

$$u(1, t) = s(t), \qquad t \geqslant 0. \tag{1.3}$$

A standard pseudospectral method [5] for solving (1.1)–(1.3) is based on interpolating the solution at the extremal points

$$x_i = \cos\left(\frac{i\pi}{N}\right), \qquad i = 0, \ldots, N, \tag{1.4}$$

of the Nth-order Chebyshev polynomial

$$T_N(x) = \cos(N \arccos(x)). \tag{1.5}$$

Using this method for space discretization and a standard explicit scheme (e.g., Runge–Kutta) for time discretization, one encounters a stability condition which has to satisfy [5]

$$\Delta t = O(N^{-2}). \tag{1.6}$$

This restriction is very stringent and forces the user to march in time steps which, in many cases, are much below the time step dictated by the physics of the problem. A way of overcoming this annoying phenomenon is to use implicit time marching techniques. Since the pseudospectral differentiation matrix is dense, the resulting algorithm is highly time consuming. Therefore, we would like to find a way to advance explicitly in time with a less restrictive stability condition. Our research is aimed at this target.

Chebyshev points (1.4) are bunched near the boundaries with minimal spacing of $O(N^{-2})$. Since the pseudospectral method is global, there is no direct relation between the minimal spacing and the stability condition as in finite-difference method [9]. Nevertheless, numerical experience and heuristic reasoning led us to "blame" the superfine grid near the boundaries for the severe stability condition (1.6). When there are sharp gradients near the boundaries, the clustering of points is needed for resolution and the small time step can also be anticipated by physical reasonings. But when the high gradients are elsewhere, or if the solution is evenly smooth, there seems to be no justification in putting more points near the boundary. If we do so, it is only because nonuniform distribution of points is essential for

* This research was supported by the Air Force Office of Scientific Research Grant No. 85-0303. Additional support was provided by the National Aeronautics and Space Administration under NASA Contract No. NAS1-18107.

0021-9991/93 $5.00

polynomial approximation. Thus, we are led to the conclusion that the numerical tool we are using (polynomial interpolation) is inappropriate in these cases.

In [2], Bayliss *et al.* describe a physical model with very sharp gradients. In order to overcome the numerical difficulties, they have designed an algorithm where the problem is transformed so as to minimize some functional. In our research, we use a similar transformation approach. The collocation points are chosen as

$$x_i = g(y_i; \alpha), \qquad -1 \leqslant x_i \leqslant 1, \quad i = 0, ..., N, \qquad 0 \leqslant \alpha < 1, \tag{1.7}$$

where

$$y_i = \cos(i\pi/N), \qquad i = 0, ..., N, \tag{1.8}$$

α is a parameter, and $g(y; \alpha)$ is a "stretching function." By a proper choice of the parameter α we increase the minimal spacing near the boundaries such that

$$\Delta x_{\min} = O(N^{-1}). \tag{1.9}$$

Consequently, we are able to advance in time with the favorable stability condition

$$\Delta t = O(N^{-1}). \tag{1.10}$$

Moreover, it is shown that, as $N \to \infty$, one needs only two points per wavelength for resolution (as in the Fourier method) and not π points as in the Chebyshev case [5]. Thus, fewer points are needed to model the PDE (a saving of almost 40%). It is well known that the matrices involved in Chebyshev (Legendre) spectral methods are far from being normal. Thus, the algorithms which result can be very sensitive to roundoff errors [13]. The spectral method described in the present paper does not suffer from this drawback since the non-normality of the matrices involved is much less pronounced.

The transformation function is given in Section 2. In Section 3 we present the resolution analysis which also reveals the approximation subspace on which the solution is projected. In order to efficiently implement the algorithm, it is important to choose the appropriate parameter α and this subject is discussed in Section 4. In Section 5 we present a more general transformation which gives additional flexibility to the new interpolation method. The paper is concluded in Section 6 in which we present numerical results.

2. MODIFIED CHEBYSHEV METHOD

Chebyshev pseudospectral solution of (1.1)–(1.3) is based on approximating the spatial derivative by analytically differentiating the interpolating polynomial. If v is an N dimensional vector which approximates $u(x)$ at the interpolation points (1.4) then the vector

$$v' = Dv \tag{2.1}$$

approximates $u'(x)$ at (1.4); D is the spatial differentiation matrix which incorporates the boundary condition (1.3). The entries of D are given in [6] ((2.1) can be accomplished by using FFTs requiring only $O(N \log N)$ operations [6]). The matrix D is very ill-conditioned, with eigenvalues scattered in the left side of the complex plane [4]. While most of the eigenvalues grow like $O(N)$, a few of them are $O(N^2)$ [4]. These extreme eigenvalues are the reason for the severe stability condition (1.6). We have to choose $\Delta t = O(N^{-2})$ so that all the eigenvalues of $\Delta t\, D$ will be included in the domain of stability of the time marching scheme.

Furthermore,

$$\Delta x_{\min} = \min_i |x_{i+1} - x_i| = 1 - \cos(\pi/N) = O(N^{-2}). \tag{2.2}$$

This phenomenon of having a domain of eigenvalues whose size is proportional to the reciprocal of the minimal spacing is typical of many differentiation matrices. Even in cases where this correspondence does not hold, as in the Legendre pseudospectral method [10], we still have to choose the time step dictated by the minimal spacing due to numerical instability whose origin is the ill-conditioning of the matrix which diagonalizes the differentiation matrix [12]. Thus, we would like to have a set of interpolating points with larger minimal spacing. We are going to attain this goal by mapping the Chebyshev points (1.8) to another set of points in $[-1, 1]$ such that the minimal spacing near the boundary is "stretched."

Let us consider the transformation

$$x = g(y; \alpha) = \frac{\text{arc sin}(\alpha y)}{\text{arc sin}(\alpha)}, \qquad x, y \in [-1, 1]. \tag{2.3}$$

Computing the derivative at the grid points x_i,

$$x_i = g(y_i; \alpha), \qquad 0 \leqslant i \leqslant N, \tag{2.4}$$

where

$$y_i = \cos(i\pi/N), \qquad 0 \leqslant i \leqslant N, \tag{2.5}$$

is accomplished by making use of the chain rule. For given $f \in C^1[-1, 1]$, we have

$$\frac{df}{dx} = \frac{1}{g'(y; \alpha)} \frac{df}{dy}. \tag{2.6}$$

Hence, we modify (2.1) to read

$$v' = ADv, \tag{2.7}$$

where A is a diagonal matrix

$$A_{ii} = \frac{1}{g'(y_i;\alpha)} \tag{2.8}$$

and

$$g'(y;\alpha) = \frac{\alpha}{\arcsin(\alpha)} \frac{1}{\sqrt{1-(\alpha y)^2}}; \tag{2.9}$$

v and v' contain the approximated values of $u(x)$ and $u'(x)$, respectively, at $x_i = g(y_i;\alpha)$. We have

LEMMA 2.1. *If x_i, $0 \leqslant i \leqslant N$, satisfy (2.4) then the minimal spacing between the points is attained near the boundaries.*

Proof. Define

$$\theta = \arccos(y). \tag{2.10}$$

Using the mean value theorem

$$\Delta x_i = x_{i+1} - x_i = \frac{dg}{d\theta}(\xi_i)\,\Delta\theta,$$
$$\theta_i \leqslant \xi_i \leqslant \theta_{i+1}, \quad 0 \leqslant i \leqslant N-1 \tag{2.11}$$

while

$$\Delta\theta = \pi/N. \tag{2.12}$$

By (2.3) and (2.10) we have

$$\frac{dg}{d\theta} = \frac{\alpha}{\arcsin(\alpha)} h(\theta), \tag{2.13}$$

where

$$h(\theta) = -\frac{\sin(\theta)}{\sqrt{1-(\alpha\cos(\theta))^2}}. \tag{2.14}$$

We have

$$h(0) = 0, \qquad h\left(\frac{\pi}{2}\right) = -1, \qquad h(\pi) = 0, \tag{2.15}$$

and

$$h'(\theta) = \frac{\cos(\theta)(\alpha^2-1)}{(1-(\alpha\cos(\theta))^2)^{3/2}} \tag{2.16}$$

is negative in $0 < \theta < \pi/2$ and positive in $\pi/2 < \theta < \pi$. Hence, $|h(\theta)|$ attains its minima at $\theta = 0, \pi$ and the result follows.

Hence

$$\Delta x_{\min} = 1 - x_1 = 1 - \frac{\arcsin(\alpha\cos(\pi/N))}{\arcsin(\alpha)}. \tag{2.17}$$

It is easily verified that the RHS of (2.17) is monotonically increasing with α, $\alpha \in (0, 1)$, and

$$\lim_{\alpha\to 1} \Delta x_{\min} = \frac{2}{N} \qquad \text{(as in Fourier case).} \tag{2.18}$$

$$\lim_{\alpha\to 0} \Delta x_{\min} = 1 - \cos\left(\frac{\pi}{N}\right) \qquad \text{(as in Chebyshev case).} \tag{2.19}$$

LEMMA 2.2. *If*

$$\alpha = 1 - \frac{c}{N^2} + O(N^{-3}), \qquad c > 0 \tag{2.20}$$

then

$$\Delta x_{\min} = \frac{2\pi}{\sqrt{\pi^2+2c}+\sqrt{2c}}\left(\frac{1}{N}\right) + O(N^{-2}). \tag{2.21}$$

Proof. Define $z = 1/N$; then

$$\Delta x_{\min} = 1 - s(z), \tag{2.22}$$

where

$$s(z) = \frac{\arcsin(g_1(z))}{\arcsin(g_2(z))}, \tag{2.23}$$

$$g_1(z) = (1-cz^2)\cos(\pi z) + O(z^3), \tag{2.24}$$

$$g_2(z) = (1-cz^2) + O(z^3). \tag{2.25}$$

We have $s(0) = 1$ and

$$s'(0_+) = \frac{2}{\pi}\lim_{z\to 0_+}\left(\frac{g_1'}{\sqrt{1-g_1^2}} - \frac{g_2'}{\sqrt{1-g_2^2}}\right). \tag{2.26}$$

Using l'Hôpital's rule it is easily verified that

$$s'(0_+) = \frac{-2}{\pi}\left(\sqrt{-g_1''(0)} - \sqrt{-g_2''(0)}\right)$$
$$= \frac{-2}{\pi}\left(\sqrt{\pi^2+2c} - \sqrt{2c}\right)$$
$$= \frac{-2\pi}{\sqrt{\pi^2+2c}+\sqrt{2c}}. \tag{2.27}$$

Since

$$\Delta x_{\min} = 1 - s(z) = 1 - [s(0) + s'(0_+)z + O(z^2)] \quad (2.28)$$

the result follows.

Based on Lemma 2.2 we conjecture that the time restriction of the new interpolation method with α satisfying (2.20) is $O(N^{-1})$. Numerical results reported in Section 6 assist this conjecture.

3. RESOLUTION ANALYSIS

Let

$$f_1(x) = \cos(r\pi x), \qquad -1 \leqslant x \leqslant 1, \quad (3.1)$$

$$f_2(x) = \sin(r\pi x), \qquad -1 \leqslant x \leqslant 1 \quad (3.2)$$

be functions whose derivative we want to approximate (r is a real number which indicates the wave number). Substituting (2.3) in (3.1) and (3.2) we have

$$f_1(x) = \tilde{f}_1(y) = \cos[m \arcsin(\alpha y)] \quad (3.3)$$

$$f_2(x) = \tilde{f}_2(y) = \sin[m \arcsin(\alpha y)], \quad (3.4)$$

where

$$m = \frac{r\pi}{\arcsin(\alpha)}. \quad (3.5)$$

In the appendix we show that for m even

$$\cos(m\psi) = (-1)^{m/2}\, T_m(\sin(\psi)), \quad (3.6)$$

for m odd

$$\sin(m\psi) = (-1)^{(m-1)/2}\, T_m(\sin(\psi)). \quad (3.7)$$

Hence, using (3.3)–(3.5),

$$\tilde{f}_1(y) = (-1)^{m/2}\, T_m(\alpha y) \qquad (m \text{ even}) \quad (3.8)$$

and

$$\tilde{f}_2(y) = (-1)^{(m-1)/2}\, T_m(\alpha y) \qquad (m \text{ odd}). \quad (3.9)$$

$T_m(\alpha y)$ is a polynomial in y; therefore, interpolating at $N+1$ points, $m \leqslant N$, will result in the function itself. Hence, the new algorithm is exact for the following $N+1$ functions (N even):

$$1, \cos(2px), \cos(4px), \ldots, \cos(Npx),$$
$$\sin(px), \sin(3px), \ldots, \sin((N-1)px), \quad (3.10)$$

where

$$p = \arcsin(\alpha). \quad (3.11)$$

The set of functions (3.10) span the approximation subspace. Observe that the basis functions are *nonperiodic*. An elaborate discussion of this subspace will be given in a future paper.

Let us clarify now what we mean by resolution. If Chebyshev expansion of a function $h(y)$ is

$$h(y) = \sum_{k=0}^{\infty} \frac{1}{c_k} a_k T_k(y),$$
$$c_0 = 2,\ c_k = 1 \qquad \text{for} \quad k \neq 0, \quad (3.12)$$

and there is K such that a_k decreases rapidly when k increases beyond K, then we say that $h(y)$ is resolved by K terms. Since Chebyshev expansion is qualitatively similar to interpolation at Chebyshev points (1.8), it is equivalent to saying that we need K points in order to resolve $h(y)$ by interpolation.

We speculate that

Conjecture. The function $T_m(\alpha y)$ is resolved by $M+1$ terms, where

$$M = [\alpha m]. \quad (3.13)$$

The reasoning for this conjecture goes as follows: Let

$$T_m(\alpha y) = \sum_{k=0}^{m} \frac{1}{c_k} a_k^m T_k(y),$$
$$c_0 = 2,\ c_k = 1 \qquad \text{for} \quad k \neq 0; \quad (3.14)$$

then

$$a_k^m = \frac{2}{\pi} \int_{-1}^{1} \frac{T_m(\alpha y)\, T_k(y)}{\sqrt{1-y^2}}\, dy. \quad (3.15)$$

Chebyshev polynomials satisfy the recurrence relation

$$T_{n+1}(x) = 2xT_n(x) - T_{n-1}(x). \quad (3.16)$$

Hence

$$a_k^m = \frac{2}{\pi} \int_{-1}^{1} \frac{\{2\alpha y T_{m-1}(\alpha y) - T_{m-2}(\alpha y)\}\, T_k(y)}{\sqrt{1-y^2}}\, dy, \quad (3.17)$$

$$m \geqslant 2 \quad (3.18)$$

$$a_0^0 = 0, \qquad a_0^1 = 0, \qquad a_1^1 = \alpha.$$

By (3.16), $2yT_k(y) = T_{k+1}(y) + T_{k-1}(y)$ which implies the relation

$$a_k^m = c_k\alpha(a_{k-1}^{m-1} + a_{k+1}^{m-1}) - a_k^{m-2},$$
$$k \geq 0, \quad m \geq 2 \quad (a_{-1}^{m-1} = 0). \tag{3.19}$$

We have programmed (3.19) with initial values (3.18) and ran it for many values of m and α and have always observed that when $k \leq M$, a_k^m are nondecreasing. Once k is greater then M, a_k^m decreases very rapidly.

Therefore, using (3.5), the maximal wave number which can be resolved by the new method is

$$r_{\max} = \frac{N \arcsin(\alpha)}{\pi\alpha}. \tag{3.20}$$

Observe that

$$\lim_{\alpha \to 1} r_{\max} = N/2 \qquad \text{(as in Fourier case)}. \tag{3.21}$$

$$\lim_{\alpha \to 0} r_{\max} = N/\pi \qquad \text{(as in Chebyshev case)}. \tag{3.22}$$

Thus, by (3.21), asymptotically, two points per wavelength are needed for resolution.

We have shown that for r satisfying (3.5) with m even (odd), $\tilde{f}_1(y)$ ($\tilde{f}_2(y)$) is a polynomial in y. Let us discuss now the resolution of a general trigonometric function

$$f(x) = \exp(ir\pi x). \tag{3.23}$$

We have

$$\tilde{f}(y) = f(g(y;\alpha))$$
$$= \exp\left[i\frac{r\pi}{\arcsin(\alpha)} \arcsin(\alpha y)\right]. \tag{3.24}$$

If

$$\frac{r\pi}{\arcsin(\alpha)} = k + \beta, \qquad 0 \leq \beta \leq 1, \ k \text{ integer} \tag{3.25}$$

then

$$\tilde{f}(y) = \exp[ik \arcsin(\alpha y)]$$
$$\times \exp[i\beta \arcsin(\alpha y)]. \tag{3.26}$$

Let us assume, without loss of generality, that k is even, then by Lemmas A.1, A.2,

$$\tilde{f}(y) = (-1)^{k/2}\,(T_k(\alpha y) - i\sqrt{1-(\alpha y)^2}\,P_{k-1}(\alpha y))$$
$$\times (\sqrt{1-(\alpha y)^2} + i\alpha y)^{\beta}. \tag{3.27}$$

Resolution of $\tilde{f}(y)$ by interpolation is influenced by the degree k of the polynomials involved and by the singularities at $\pm 1/\alpha$. The degree of the interpolating polynomial has to be at least αk but the asymptotic rate of convergence depends only on the singularites. The relevant theory is presented below in greater generality.

Let $f(x)$ be an analytic function in $E \supset [-1, 1]$. Since $g'(y;\alpha)$ (2.9) has singularities at $y = \pm 1/\alpha$, so does $\tilde{f}(y) = f(g(y;\alpha))$. Define

$$B = \left(-\frac{1}{\alpha}, \frac{1}{\alpha}\right) \tag{3.28}$$

and assume that α is close enough to one so that

$$B \subset g^{-1}(E). \tag{3.29}$$

Thus, $\tilde{f}(y)$ is analytic in B. The rate of convergence of polynomial interpolation at Chebyshev points is based on the following theory from [14]: Let K be a bounded continuum in C (complex plane) such that K^c = the complement K is *simply connected in the extended plane and contains the* point at infinity. For such K there exists a conformal mapping $\Psi(w)$ which maps the complement of the unit disc *onto* K^c [14]. Let $\Phi(z)$ be the inverse of $\Psi(w)$ and

$$B_t = \{z : |\Phi(z)| = t\} \qquad (t > 1) \tag{3.30}$$

denote the level curves in K^c.

THEOREM 2.1. *Suppose $t > 1$ is the largest number such that $f(z)$ is analytic inside B_t. The interpolating polynomials $P_n(z)$ with interpolating points z_i^n that are uniformly distributed on K then satisfy*

$$\lim_{n \to \infty} \max_{z \in K} |f(z) - P_n(z)|^{1/n} = 1/t. \tag{3.31}$$

Since Chebyshev points satisfy the definition of uniformally distributed points on $[-1, 1]$ [14], the asymptotic rate of convergence can be computed by making use of this theorem. We choose $K = [-1, 1]$, and the relevant conformal mapping is given by [8]

$$\Phi(y) = y \pm \sqrt{y^2 - 1}. \tag{3.32}$$

Assume now that if $\tilde{f}(y)$ has additional singularities in the complex plane then α is close enough to one so that the largest t corresponds to the singular points $\pm 1/\alpha$. Thus

$$t = \frac{1 + \sqrt{1-\alpha^2}}{\alpha} \tag{3.33}$$

and the asymptotic rate of convergence is

$$\frac{1}{t}=\frac{1-\sqrt{1-\alpha^2}}{\alpha}. \tag{3.34}$$

Hence, by interpolating at $N+1$ points, we have

$$\max_{z\in K}|f(z)-P_N(z)|=c\varepsilon, \tag{3.35}$$

where

$$\varepsilon=\left(\frac{1-\sqrt{1-\alpha^2}}{\alpha}\right)^N \tag{3.36}$$

and c is a constant which depends on f but does not depend on N or y.

4. ON THE CHOICE OF THE PARAMETER α

For a predetermined degree N we would like to choose the appropriate parameter α. Given below are three constructive ways for choosing α, based on different considerations.

Resolution considerations. Sometimes we have an idea on the maximal wave number ($r_{\max}$) which we want to resolve. For instance, if there is a source term in our equations with known band of frequencies. In this case we will solve (3.20) for α. Assuming that α is close to one we can simplify (3.20) and use instead

$$\alpha=\sin\left(\frac{\pi r_{\max}}{N}\right), \qquad r_{\max}<\frac{N}{2}. \tag{4.1}$$

If

$$r_{\max}=\frac{N}{2}-j, \qquad j\ll\frac{N}{2} \tag{4.2}$$

then

$$\alpha=\sin\left(\frac{\pi}{2}-\frac{j}{N}\pi\right)=\cos\left(\frac{j}{N}\pi\right), \tag{4.3}$$

j being the number of modes which we "give up" resolving. Expanding in Taylor series

$$\alpha=1-\frac{1}{2}j^2\left(\frac{\pi}{N}\right)^2+\cdots \tag{4.4}$$

which satisfies (2.20) and by using (4.4) and (2.21) we obtain

$$\Delta x_{\min}=\frac{2}{j+\sqrt{j^2+1}}\frac{1}{N}+O(N^{-2}). \tag{4.5}$$

Remark 4.1. Resolution analysis is closely related to maximal spacing analysis. By the sampling theorem we know that for any sampling interval Δ, there is maximal mode w_c called the Nyquist critical frequency and is given by $w_c=1/\Delta$. For the Fourier method we have $\Delta x=2/N$; hence the maximal mode which can be resolved is $N/2$. Similarly, in the Chebyshev case, $\Delta x_{\max}=\pi/N$ and the maximal mode is N/π which is equivalent to stating that π points per wavelength are needed for resolution. This result is given also in [5], based on expanding the trigonometric functions in Chebyshev polynomials. By Lemma 2.1 we obtain that for the transformed interpolating points, the maximal spacing is attained in the center of the interval. Therefore,

$$\Delta x_{\max}=g\left[\cos\left(\frac{\pi}{2}-\frac{\pi}{N}\right)\right]-g(0)$$

$$=\frac{\arcsin[\alpha\sin(\pi/N)]}{\arcsin(\alpha)}. \tag{4.6}$$

Substituting (4.3) in (4.6) we obtain

$$\frac{1}{\Delta x_{\max}}\approx\frac{N}{2}-j, \qquad N\gg j, \tag{4.7}$$

similar to (4.2).

Accuracy considerations. For given ε and N, we can solve (3.36) for α and obtain an explicit expression,

$$\alpha=\frac{2}{t+t^{-1}}, \qquad t=\varepsilon^{-1/N}. \tag{4.8}$$

To examine the minimal spacing dictated by this choice, we expand α in Taylor series

$$\alpha=1-\frac{1}{2}\ln^2(\varepsilon)\left(\frac{1}{N}\right)^2+O(N^{-2}). \tag{4.9}$$

The expansion (4.9) is of the form (2.20); using it and (2.21) we obtain

$$\Delta x_{\min}=\frac{2\pi}{(|\ln(\varepsilon)|+\sqrt{\pi^2+\ln^2(\varepsilon)})}\frac{1}{N}$$
$$+O(N^{-2}). \tag{4.10}$$

The agreement between ε and the computed accuracy will depend on the constant c (3.35). Observe that there is a "give and take" relation between resolution and accuracy. By decreasing $r_{\max}$, α is decreased (4.1) and, therefore, ε is becoming smaller (3.36). Hence, by sacrificing the resolution of the high modes, we obtain, in return, higher accuracy on the rest of the modes (see numerical results in Section 6).

Adaptive approach. We have described above two formulas which give explicit expressions for α. One can also consider a third approach, an adaptive algorithm for computing α. Observing (2.6) we can regard the method described in this paper as a "preconditioning" one. For a given function, we are looking for a parameter α such that after the transformation, $\tilde{f}(y)$ can be approximated by Chebyshev polynomials expansion with a minimal number of terms. One can consider the tail of the series of pseudospectral Chebyshev coefficients as a criterion for choosing α. Since, by stability considerations we would like α to be as large as possible, the adaptive algorithm should find

$$\alpha_{\max} = \max\left\{\alpha \left| \frac{\sum_{i=N-k}^{N} |a_i(\alpha)|}{\sum_{i=0}^{N} |a_i(\alpha)|} < \varepsilon_0,\ k \ll N \right.\right\}, \tag{4.11}$$

where ε_0 is a given tolerance and a_i are the computed Chebyshev coefficients. When the adaptive approach is implemented in time dependent problems, the search for an optimal α should restart whenever the solution behavior has been changed significantly.

5. NONSYMMETRIC TRANSFORMATION

The transformation function (2.3) is symmetric. The interpolating points (2.4) are distributed symmetrically around the origin. When there is a boundary layer on one side of the domain, we would like to have the flexibility of putting more points on this side. To this end we modify the transformation (2.3) and take

$$x = g(y; \alpha, \beta) = \frac{1}{a}(\tilde{g}(y; \alpha, \beta) - b), \tag{5.1}$$

where

$$\tilde{g}(y; \alpha, \beta) = \arcsin\left(\frac{2\alpha\beta y + \alpha - \beta}{\alpha + \beta}\right) \tag{5.2}$$

and

$$a = \tfrac{1}{2}\{\tilde{g}(1; \alpha, \beta) - \tilde{g}(-1; \alpha, \beta)\} \tag{5.3}$$

$$b = \tfrac{1}{2}\{\tilde{g}(1; \alpha, \beta) + \tilde{g}(-1; \alpha, \beta)\}. \tag{5.4}$$

For the derivative we have

$$\frac{1}{g'(y; \alpha, \beta)} = \frac{a}{\sqrt{\alpha\beta}}\sqrt{(1-\alpha y)(1+\beta y)} \tag{5.5}$$

and the parameters α and β control the distribution of interpolation points near $x = 1$ and $x = -1$, respectively. An elaborate discussion of this transformation will be given in a future paper.

6. NUMERICAL RESULTS

The following notations are used in this section:

N = number of interpolating points.

E = relative error of the derivative in the maximum norm.

j = number of unresolved modes (4.2).

y_i = Chebyshev interpolating points (2.5).

z_i = check points,

$$z_i = g(\cos(y_{i+1/2}; \alpha)), \qquad 0 \leqslant i \leqslant N-1. \tag{6.1}$$

In the first table we present the spectral radius ρ of AD (2.7), where α is given by (4.3). The spectral radius of the Chebyshev pseudospectral differentiation operator D is given in the last column. Using the new method for time dependent problems we have observed that

$$\frac{\Delta t(\text{new method})}{\Delta t(\text{Chebyshev})} \approx \frac{\rho(D)}{\rho(AD)}. \tag{6.2}$$

Thus, from Table I we see that for $N = 128$, for example, the time step restriction of the new algorithm is almost eight times larger then the one used in a standard Chebyshev discretization.

TABLE I

Spectral Radius

j	N	α	$\rho(AD)$	$\rho(D)$
1	16	0.9808	18.927	23.560
1	32	0.9952	42.897	91.559
1	64	0.9987	92.286	363.779
1	128	0.9997	192.165	1452.706
2	16	0.9239	17.934	23.560
2	32	0.9808	41.061	91.559
2	64	0.9952	89.957	363.779
2	128	0.9988	189.454	1452.706
3	16	0.8312	18.624	23.560
3	32	0.9569	44.600	91.559
3	64	0.9892	97.846	363.779
3	128	0.9973	204.997	1452.706

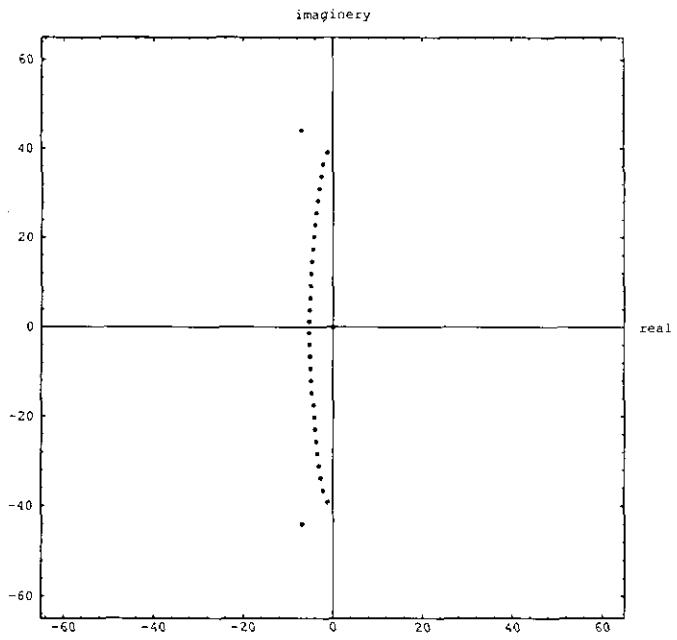

FIG. 1. Eigenvalues of AD, $j=3$, $N=32$.

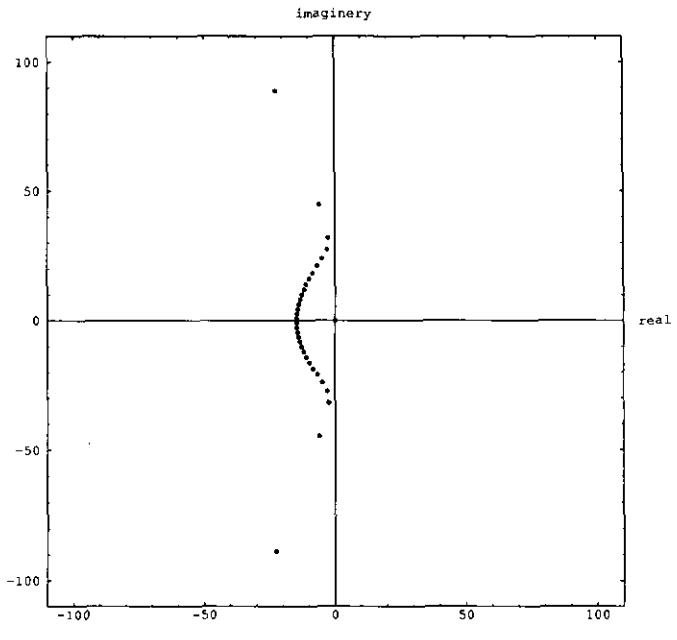

FIG. 3. Eigenvalues of D, $N=32$, double precision (16 digits).

The eigenvalues of AD lie in the left side of the complex plane (Figs. 1, 2). Carrying out the computations in single precision (eight digits) or double precision (16 digits) gave identical results. Hence, the differentiation matrix is not sensitive to roundoff errors. It is in contrast to the Chebyshev case (Figs. 3, 4), where, due to the severe non-normality of the matrix, the eigenvalues distribution depends strongly on the machine accuracy [12]. A useful measure of the normality of the matrix AD is the size of the condition number $\kappa(T)=\|T\|\,\|T^{-1}\|$, where T is the matrix whose columns are the normalized eigenvectors of AD. In Table II we give the condition numbers for several values of N and j ($j=N/2$ is the Chebyshev case ($A=I$)).

The super sensitivity of the eigenvalues computation in the Chebyshev case is more pronounced in the following problem:

$$u_t + xu_x = 0, \qquad -1 < x < 1, \quad t \geqslant 0, \tag{6.3}$$

$$u(x, 0) = u^0(x), \qquad -1 < x < 1. \tag{6.4}$$

In this case, even though the exact eigenvalues are $0, -1,$

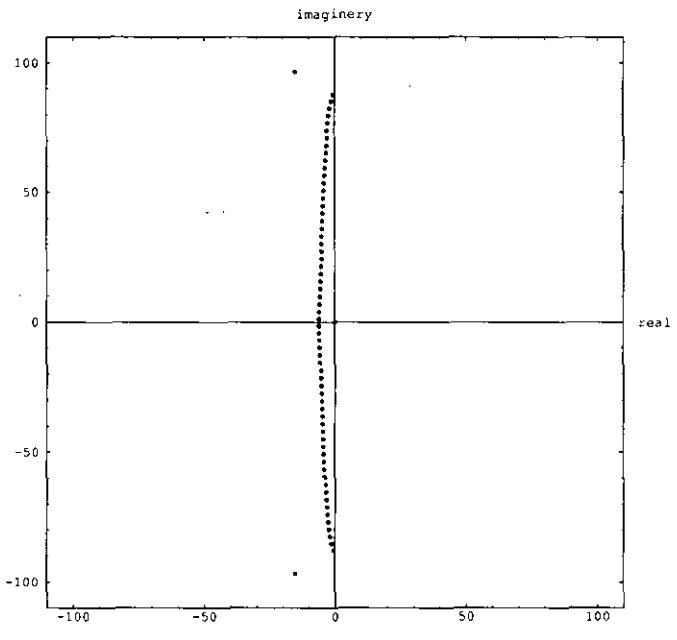

FIG. 2. Eigenvalues of AD, $j=3$, $N=64$.

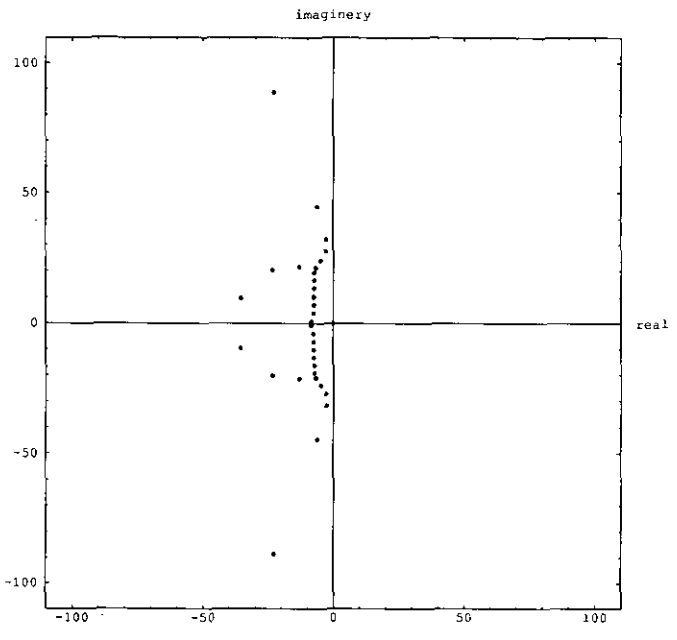

FIG. 4. Eigenvalues of D, $N=32$, singe precision (8 digits).

TABLE II

Condition Number

N	$j=1$	$j=2$	$j=3$	$j=N/2$
8	$6.7E+01$	$2.4E+02$	$6.5E+02$	$7.7E+02$
16	$1.5E+02$	$2.0E+03$	$8.8E+03$	$1.1E+06$
32	$8.9E+02$	$1.2E+04$	$8.8E+04$	$2.8E+12$
64	$3.1E+03$	$5.0E+04$	$7.9E+05$	$1.1E+15$

$-2, ..., -N$ (with eigenvectors: $1, x, x^2, ..., x^N$), the computed eigenvalues are $O(N^2)$ (Fig. 5). On the other hand, using the new method, the relevant eigenvalues are not sensitive to roundoff errors and are $O(N)$ (Figs. 6, 7).

The results given in Tables III and IV demonstrate the resolution and accuracy properties of the new algorithm and clarify the "give and take" relation between the two as mentioned in Section 4. We applied the new differentiation algorithm to the trigonometric functions

$$u_k(x) = \cos(k\pi x), \qquad 1 \leqslant k \leqslant 16, \tag{6.5}$$

and obtained approximations v_k', $k = 1, ..., 16$; α is given by (4.3). Corresponding results for the Chebyshev method are shown in the last column. In the last row we have printed ε as given by (3.36). The resolution property of $N/2 - j$ modes (4.2), (4.7) is clearly demonstrated in the tables. As j increases, so does the accuracy of the modes resolved. As shown in Section 3, the new method should be exact if

$$m = \frac{2kN}{N-2j} \tag{6.6}$$

is an even integer. This explains the high accuracy exhibited in relevant entries of Tables III and IV. Comparing Table III to Table IV we see that the accuracy by which the low modes are resolved is almost the same. The effect of increasing N is in the number of modes resolved with accuracy imposed by the choice of j.

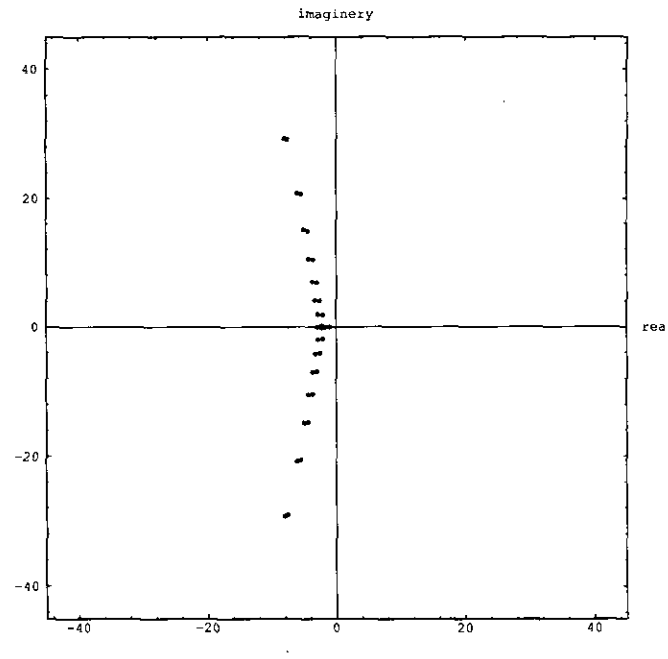

FIG. 6. Eigenvalues of the matrix related to modified Chebyshev approximation of (6.3), (6.4); $N = 32$.

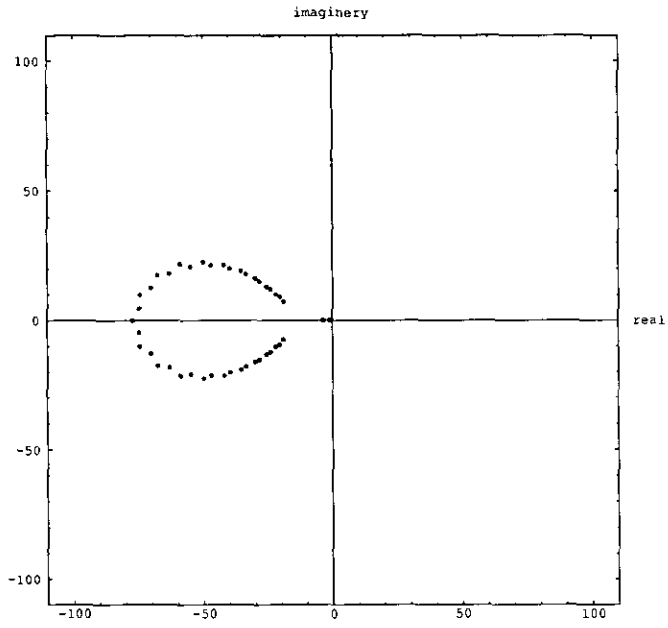

FIG. 5. Eigenvalues of the matrix related to Chebyshev approximation of (6.3), (6.4); $N = 64$; single precision.

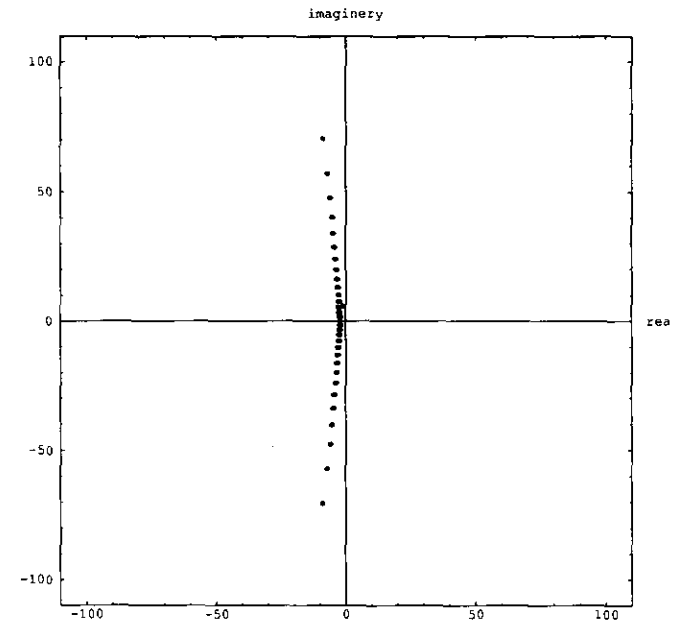

FIG. 7. Eigenvalues of the matrix related to modified Chebyshev approximation of (6.3), (6.4); $N = 64$.

TABLE III

$N = 32$

k	$E(j=1)$	$E(j=2)$	$E(j=3)$	$E(j=4)$	E_{chb}
1	9.35E−03	7.14E−04	3.78E−05	1.57E−06	1.57E−12
2	1.86E−02	1.35E−03	6.23E−05	1.77E−06	5.83E−13
3	2.84E−02	1.82E−03	5.84E−05	1.66E−06	3.29E−13
4	3.70E−02	2.02E−03	2.06E−05	2.97E−06	5.65E−11
5	4.76E−02	1.88E−03	5.14E−05	4.42E−06	4.41E−08
6	5.44E−02	1.25E−03	1.42E−04	3.90E−14	7.56E−06
7	6.29E−02	3.19E−14	2.10E−04	1.36E−05	4.14E−04
8	7.04E−02	2.04E−03	1.68E−04	2.93E−05	9.33E−03
9	7.76E−02	5.07E−03	1.54E−04	4.10E−14	9.34E−02
10	8.36E−02	9.26E−03	1.07E−03	2.46E−04	4.52E−01
11	8.58E−02	1.48E−03	3.12E−03	1.16E−03	8.94E−01
12	8.46E−02	2.10E−02	6.60E−03	3.01E−14	1.56E+00
13	7.82E−02	2.48E−02	3.52E−14	3.75E−01	1.72E+00
14	5.70E−02	4.07E−14	7.39E−01	1.32E+00	1.70E+00
15	3.87E−14	1.25E+00	1.79E+00	1.86E+00	1.34E+00
16	1.69E+00	1.92E+00	1.76E+00	1.79E+00	1.63E+00
ε	4.32E−02	1.79E−03	6.99E−05	2.49E−06	—

In Tables V and VI we present mesh refinement charts for the functions

$$f_1(x) = \frac{0.05}{x^2 + 0.05}, \tag{6.7}$$

$$f_2(x) = \frac{\exp(2x)}{2 + \cos(15x)}, \tag{6.8}$$

respectively. In Table V, α is given by (4.3) with $j = 3$. Observe the fast convergence up to $N = 64$. The error is not decreasing beyond this points, since all the modes have been resolved to the accuracy enforced by the choice of j. In Table VI, α is computed by (4.8) with $\varepsilon = 1.E-0.5$. The results for Chebyshev method are given in the last column.

TABLE IV

$N = 64$

k	$E(j=1)$	$E(j=2)$	$E(j=3)$	$E(j=4)$	E_{chb}
1	4.55E−03	3.53E−04	2.04E−05	1.04E−06	3.49E−11
3	1.36E−02	1.03E−04	5.53E−05	2.49E−06	7.16E−12
5	2.26E−02	1.60E−03	7.29E−05	2.26E−06	3.50E−12
7	3.16E−02	1.99E−03	6.35E−05	1.99E−13	1.85E−12
9	4.04E−02	2.13E−03	2.14E−05	3.53E−06	1.02E−12
11	4.90E−02	1.93E−03	5.26E−05	6.13E−06	2.15E−12
13	5.74E−02	1.26E−03	1.47E−04	4.12E−06	1.55E−08
15	6.52E−02	6.58E−03	2.32E−04	6.77E−06	1.48E−05
17	7.25E−02	1.99E−03	2.44E−04	2.76E−05	2.62E−03
19	7.89E−02	4.89E−03	6.26E−05	4.56E−05	9.76E−02
21	8.38E−02	8.91E−03	5.40E−04	5.81E−14	6.61E−01
23	8.66E−02	1.42E−03	1.96E−03	3.12E−04	1.78E+00
25	8.57E−02	2.07E−03	4.94E−03	1.53E−03	1.76E+00
27	7.85E−02	2.72E−03	1.01E−02	4.48E−03	1.86E+00
29	5.82E−02	2.46E−02	9.01E−14	7.12E−01	1.62E+00
31	1.48E−13	1.51E+00	2.03E+00	1.91E+00	1.77E+00
ε	4.32E−02	1.84E−03	7.80E−05	3.21E−06	—

TABLE V

Mesh Refinement Chart, $f_1(x) = 0.05/(x^2 + 0.05)$

N	α	$E(j=3)$	E_{chb}
16	0.83147	9.394E−02	1.777E−01
32	0.95694	1.019E−03	9.281E−03
64	0.98918	1.507E−06	1.486E−05
128	0.99729	1.794E−06	8.845E−11
256	0.99932	1.939E−06	9.923E−11

We have solved the model problem described in the Introduction, (1.1)–(1.3), and the results are reported in Table VII. The solution is computed at $t = 1$ using fourth-order Runge–Kutta as a time-marching algorithm. The initial and boundary conditions are

$$u^0(x) = [x \exp^{-(x-1)^2} \cos(m\pi x) - (-1)^m]^4, \tag{6.9}$$

$$u(1, t) = s(t) = 0, \tag{6.10}$$

respectively. The numerical solution is compared to the exact solution

$$u(x, t) = \begin{cases} 0, & x + t \geqslant 1 \\ [(x+t) \exp^{-(x+t-1)^2} \cos[m\pi(x+t)] - (-1)^m]^4, \\ & x + t \leqslant 1. \end{cases} \tag{6.9}$$

The results presented in the table provide a comparison between the new method, where α is computed by (4.3) with $j = 1$, and the standard Chebyshev method; *nsteps* is the number of time steps. For $m = 6$ we needed 91 points, in the Chebyshev case, in order to achieve the accuracy given in the last column. For stability we had to use 1300 time steps. Taking smaller Δt would not decrease the error as shown in the second row. Using the new algorithm, we took only 65 points; 80 time steps were sufficient for stability. In order to obtain accuracy close to the one we had in the Chebyshev case, 200 time steps were needed. Reducing Δt beyond this

TABLE VI

Mesh Refinement Chart, $f_2(x) = \exp(2x)/(2 + \cos(15x))$

N	α	$E(\varepsilon = 1.E-05)$	E_{chb}
16	0.80761	1.853E−01	1.717E−01
32	0.94208	9.007E−02	6.461E−02
64	0.98452	2.298E−03	9.032E−03
128	0.99603	1.968E−06	5.774E−05
256	0.99899	6.344E−06	1.669E−09

TABLE VII

Time-Dependent Problem (1.1)–(1.3)

m	N	α	*nsteps*	max(|E|)/max(|u|)
6	91	0	1300	8.59E−03
6	91	0	2600	8.53E−03
6	65	0.9988	80	1.79E−01
6	65	0.9988	200	7.08E−03
6	65	0.9988	300	5.64E−03
12	181	0	5200	5.32E−03
12	129	0.9997	200	2.22E−01
12	129	0.9997	600	5.71E−03

point would not reduce the error significantly as shown by the fifth row. In the next set of experiments we took $m = 12$. In both cases, we had to double the number of points in order to resolve the solution. The results are provided in the rest of the table.

In order to show that the new algorithm is insensitive to the smoothness of the solution we have solved (1.1)–(1.3) with $u^0(x) = (x+1)(x-1)$, $s(t) = 0$. The exact solution is only in C^1. As before, fourth-order Runge–Kutta is the time integrator and the numerical solution is computed at $t = 1$. The results are reported in Table VIII.

Lamb Problem

This is a problem of wave propagation in a uniform and isotropic elastic two-dimensional halfspace subjected to a point source applied in the vicinity of the free surface. This problem is numerically challenging because of the presence of Rayleigh surface waves around the free surface. The calculation of these waves requires an accurate representation of the boundary conditions.

Let x and y denote horizontal and vertical cartesian coordinates, respectively, and t, the time variable. The system of equations to be solved is

$$\frac{\partial V_x}{\partial t} = \frac{1}{\rho}\left(\frac{\partial \sigma_{xx}}{\partial x} + \frac{\partial \sigma_{xy}}{\partial y}\right) + f_x \tag{6.11}$$

$$\frac{\partial V_y}{\partial t} = \frac{1}{\rho}\left(\frac{\partial \sigma_{xy}}{\partial x} + \frac{\partial \sigma_{yy}}{\partial y}\right) + f_y \tag{6.12}$$

TABLE VIII

Time-Dependent Problem (1.1)–(1.3) with Non-smooth Solution

N	α	*nsteps*	max(|E|)/max(|u|)
65	0	130	2.28E−03
129	0	520	8.06E−04
65	0.9988	40	3.88E−03
129	0.9997	80	1.61E−03

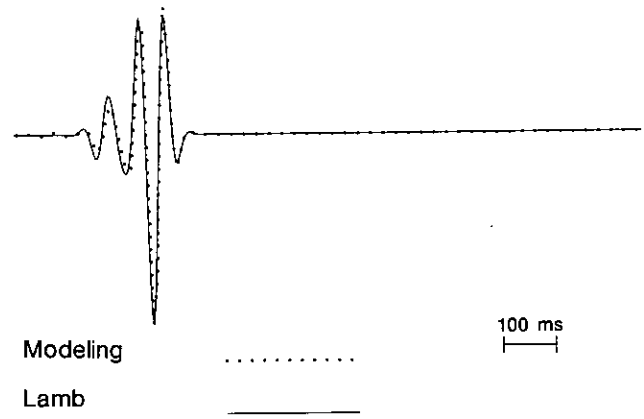

FIG. 8. Analytical and numerical horizontal displacement time history at 200_m from the source.

$$\frac{\partial \sigma_{xx}}{\partial t} = (\lambda + 2\mu)\frac{\partial V_x}{\partial x} + \lambda \frac{\partial V_y}{\partial y} \tag{6.13}$$

$$\frac{\partial \sigma_{yy}}{\partial t} = \lambda \frac{\partial V_x}{\partial x} + (\lambda + 2\mu)\frac{\partial V_y}{\partial y} \tag{6.14}$$

$$\frac{\partial \sigma_{xy}}{\partial t} = \mu \frac{\partial V_x}{\partial y} + \mu \frac{\partial V_y}{\partial x}. \tag{6.15}$$

V_x and V_y denote, respectively, the horizontal and vertical velocities; σ_{xx}, σ_{yy}, and σ_{xy} are the stress components, f_x and f_y are the body forces, ρ is the density, and λ and μ are Lamb's constants. The system is the same as the one used by Bayliss *et al.* [1] for a fourth-order finite difference scheme.

During the calculations, the variables V_x, V_y, σ_{xx}, σ_{yy}, and σ_{xy} are advanced in time after specification of the body forces f_x and f_y. In this work we choose to approximate the horizontal derivative by the Fourier method, whereas for the vertical coordinate y we choose the modified Chebyshev discretization as described in this paper, using the transfor-

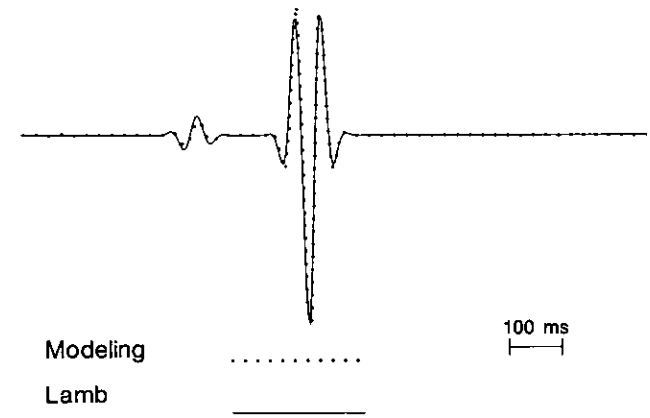

FIG. 9. Analytical and numerical horizontal displacement time history at 500_m from the source.

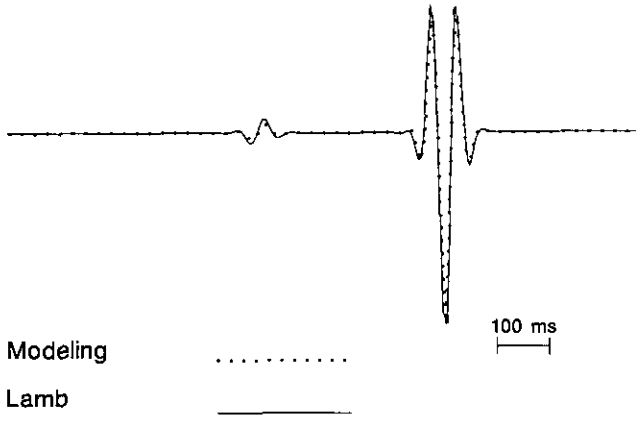

FIG. 10. Analytical and numerical horizontal displacement time history at 800_m from the source.

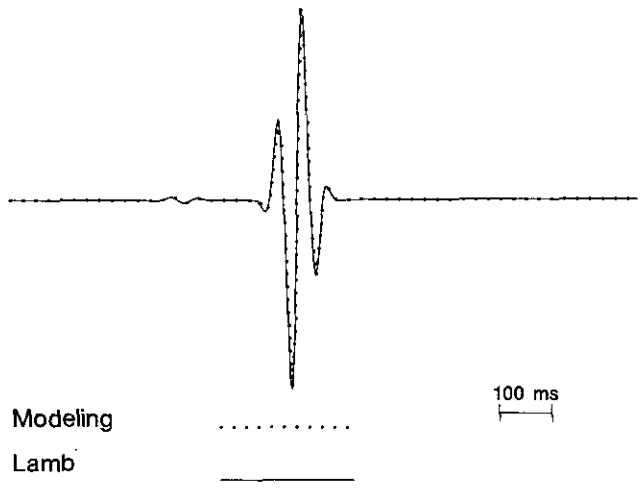

FIG. 12. Analytical and numerical vertical displacement time history at 500_m from the source.

mation function (5.1). The boundary conditions at $y=0$ is $\sigma_{yy}=\sigma_{xy}=0$, whereas for the bottom boundary $y=L$ we choose the condition that the incoming characteristics are zero [1]. In addition, an absorbing strip was applied along the lower boundary and the sides of the grid to prevent reflections or wraparound from the boundaries [7]. For the present problem the material parameters had uniform values of $\rho=1.2_{gr/cm^2}$, and P and S had velocities of $V_p=\sqrt{(\lambda+2\mu)/\rho}=2000_{m/s}$ and $V_s=\sqrt{\mu/\rho}=1155_{m/s}$, respectively. For the body forces, $f_x=0$ and $f_y=\delta(x-x_0)\,\delta(y-y_0)\,h(t)$, where $x_0=250_m$, $y_0=1.8_m$, and $h(t)$ was a band-limited Ricker wavelet with highest frequency of 40 Hz [11]. For the spatial discretization $\Delta x=\Delta y=10_m$ and the grid modification parameters (5.1) are $\alpha=0.729$ and $\beta=0.620$. The solution was advanced in time to 1_s by the fourth-order Runge–Kutta method using a time step of 0.002 s. This time step is approximately *seven times* larger than the maximum allowable time step for an ordinary Chebyshev discretization and it is approximately equal to the time step which would be used with a uniform Fourier grid from accuracy considerations (e.g., $C\,dt/dx\approx 0.4$).

Figures 8–10 present a comparison between the numerical and analytical horizontal displacement time histories at points located at respective distances of 200_m, 500_m, and 800_m from the source. A corresponding comparison of vertical displacements is presented in Figs. 11–13. As the figures show, the match between numerical and analytical solutions is virtually perfect.

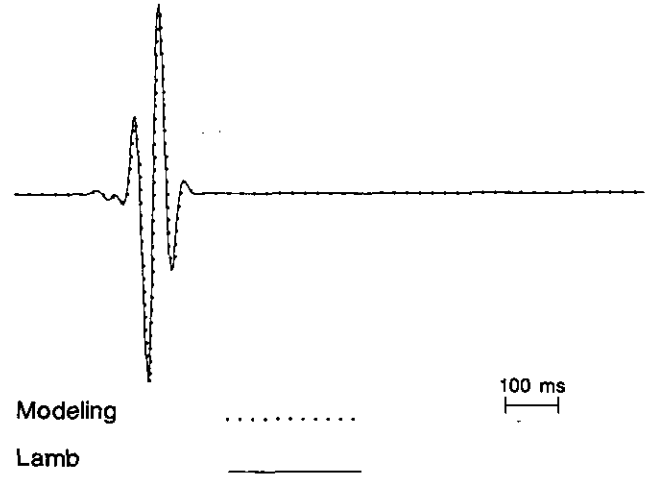

FIG. 11 Analytical and numerical vertical displacement time history at 200_m from the source.

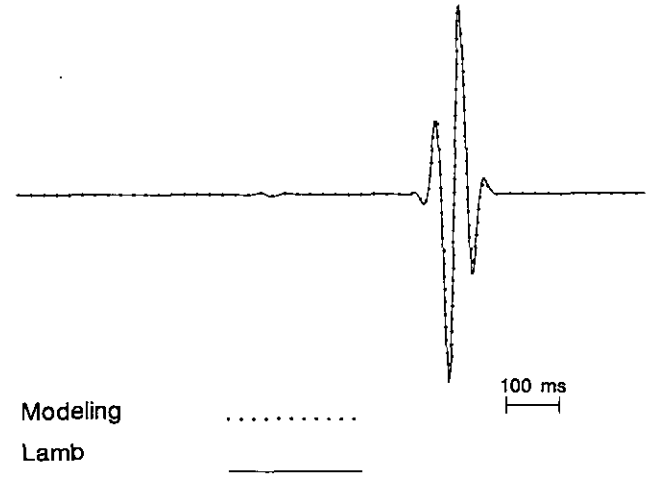

FIG. 13. Analytical and numerical vertical displacement time history at 800_m from the source.

APPENDIX

LEMMA A.1. *For m even,*

$$\cos(m\psi) = (-1)^{m/2}\, T_m(\sin(\psi)). \tag{A.1}$$

For m odd,

$$\sin(m\psi) = (-1)^{(m-1)/2}\, T_m(\sin(\psi)). \tag{A.2}$$

Proof. Chebyshev polynomials satisfy the recurrence relation

$$T_{n+1}(x) = 2xT_n(x) - T_{n-1}(x). \tag{A.3}$$

Using basic trigonometric identities, the recurrence relation and induction we obtain

$$\begin{aligned}\cos((m+2)\psi) &= 2[2\cos^2(\psi) - 1]\cos(m\psi) \\ &\quad - \cos[(m-2)\psi] \\ &= (-1)^{m/2+1}\{2[2\sin^2(\psi) - 1] \\ &\quad \times T_m(\sin(\psi)) - T_{m-2}(\sin(\psi))\} \\ &= (-1)^{m/2+1}\, T_{m+2}(\sin(\psi)).\end{aligned} \tag{A.4}$$

We will use now (A.4) to show (A.2):

$$\begin{aligned}\sin((m+2)\psi) &= \cos(2\psi)\sin(m\psi) \\ &\quad + \cos(m\psi)\sin(2\psi) \\ &= (1 - 2\sin^2\psi)(-1)^{(m-1)/2} \\ &\quad \times T_m(\sin(\psi)) + \sin(\psi) \\ &\quad \times \{\cos((m+1)\psi) \\ &\quad + \cos((m-1)\psi)\} \\ &= (-1)^{(m+1)/2}\{(2\sin^2\psi - 1) \\ &\quad \times T_m(\sin(\psi)) + \sin(\psi) \\ &\quad \times [T_{m+1}(\sin(\psi)) - T_{m-1}(\sin(\psi))]\} \\ &= (-1)^{(m+1)/2}\{2(2\sin^2(\psi) - 1) \\ &\quad \times T_m(\sin(\psi)) - T_{m-2}(\sin(\psi))\} \\ &= (-1)^{(m+1)/2}\, T_{m+2}.\end{aligned} \tag{A.5}$$

LEMMA A.2. *For m odd,*

$$\cos(m\psi) = \cos(\psi)\, P_{m-1}(\sin(\psi)) \tag{A.6}$$

and for m even,

$$\sin(m\psi) = \cos(\psi)\, Q_{m-1}(\sin(\psi)), \tag{A.7}$$

where P_{m-1}, Q_{m-1} are polynomials of degree $m-1$.

Lemma A.2 is easily verified by using trigonometric identities, induction, and the results of Lemma A.1.

REFERENCES

1. A. Bayliss, K. E. Jordan, B. J. LeMesurier, and E. Turkel, *Bull. Am. Seismol. Soc.* **6** (4), 1115 (1986).
2. A. Bayliss, D. Gottlieb, B. J. Matkowsky, and M. Minkoff, ICASE Report No. 87-67, NASA Langley Research Center, Hampton, VA 23665, 1987 (unpublished).
3. C. Canuto, M. Y. Hussaini, A. Quarteroni, and T. Zang, *Spectral Methods in Fluid Dynamics* (Springer-Verlag, Berlin/Heidelberg/New York, 1987).
4. M. Dubiner, *J. Sci. Comput.* **2**, 3 (1987).
5. D. Gottlieb and S. Orszag, *Numerical Analysis of Spectral Methods: Theory and Applications*, CBMS-NSF Regional Conference Series in Applied Mathematics (SIAM, Philadelphia, 1977).
6. D. Gottlieb and E. Turkel, ICASE Report No. 172241, NASA Langley Research Center, Hampton, VA 23665, 1983 (unpublished).
7. R. Kosloff and D. Kosloff, *J. Comput. Phys.* **63**, 363 (1986).
8. A. I. Markushevich, *Theory of Functions of a Complex Variable* (Chelsea, New York, 1977).
9. A. Solomonoff and E. Turkel, *J. Comput. Phys.* **81**, 239 (1989).
10. H. Tal-Ezer, *J. Comput. Phys.* **67**, 145 (1986).
11. H. Tal-Ezer, D. Kosloff, and Z. Koren, *Geophys. Prospect.* **35** (5), 479 (1987).
12. L. N. Trefethen and M. R. Trummer, *SIAM J. Numer. Anal.* **24**, 1008 (1987).
13. L. N. Trefethen, "Lax-Stability vs. Eigenvalues Stability of Spectral Methods," in *Numerical Methods for Fluid Dynamics III*, edited by K. W. Morton and M. J. Baines (Clarendon Press, Oxford, 1988).
14. J. L. Walsh, *Interpolation and Approximation by Rational Functions in the Complex Domain* (Am. Math. Soc., Providence, RI, 1956).